DALTON
FULL PAPER

Nickel(II) complexes with amide ligands: oxidative dehydrogenation of the amines in a tetradentate diamide–diamine ligand †

Colin L. Weeks, Peter Turner, Ronald R. Fenton * and Peter A. Lay

Centre for Heavy Metals Research, School of Chemistry, The University of Sydney, NSW 2006, Australia

Received 14th August 2001, Accepted 19th December 2001
First published as an Advance Article on the web 21st February 2002

Four complexes were prepared by the reaction of Ni(II) with three pyrrolidine based diamide–diamine ligands. The two amine groups in the ligand *N*,*N*′-bis(*S*-prolyl)-1,2-ethanediamine (*S*,*S*-bprolenH_2) were oxidatively dehydrogenated during the preparation of the Ni(II) complex in air. The reaction involved O_2 to yield a complex of a tetradentate ligand with 1-pyrroline terminal groups. The Ni(II) complex with *S*,*S*-bprolenH_2 was synthesised under oxygen-free conditions, and the Ni(II) complexes with the analogous ligands *N*,*N*′-bis(*S*-prolyl)-*R*,*R*-1,2-cyclohexanediamine (*R*,*R*-(*S*,*S*)-bprolchxnH_2) and *N*,*N*′-bis(*S*-prolyl)-1,2-benzenediamine (*S*,*S*-bprolbenH_2) were prepared in air. The complexes were characterised by X-ray crystallography, ^{1}H and ^{13}C NMR spectroscopy and IR spectroscopy. The Ni(III/II) reduction potentials of complexes with pyridyl and pyrrolidine based tetradentate diamide ligands were measured by cyclic voltammetry to assess the stability of the Ni(III) oxidation state, but did not show any correlation with the ease of ligand oxidation.

Introduction

Nickel(II) complexes with several oligopeptide ligands cause DNA cleavage in the presence of oxidants,[1–10] in some instances with sequence selectivity.[2,3,5,7,8,10] It has been postulated that Ni(III) and/or Ni(IV) complexes are among the species responsible for this DNA cleavage.[1,2,6,10] Studies on the Ni(III/II) reduction potentials of nickel–oligopeptide complexes show that an increase in the number of deprotonated amide donors lowers the Ni(III/II) reduction potential.[11,12] In the light of this, there is interest in the formation of Ni(II) complexes with amide ligands and studies of the ease of oxidation to Ni(III) analogues, and the stability of the oxidised products.

Vagg and coworkers developed a series of acyclic tetradentate ligands with two central amide groups and two terminal pyridyl groups (Fig. 1).[13,14] These ligands were used to prepare a

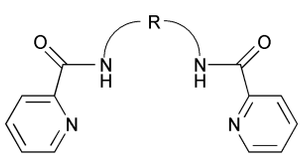

	R
I bpenH_2	-CH_2CH_2-
II bpbH_2	1,2-benzenediyl

Fig. 1 Tetradentate diamide–dipyridyl ligands

range of complexes with M(II) ions, including several Ni(II) complexes.[14–24] In this work, we report the synthesis of Ni(II) complexes with three tetradentate diamide ligands, **III–V**. These have pyrrolidine terminal groups instead of the pyridyl terminal groups used by Vagg and coworkers (Fig. 2). Ligands **III** and **IV** were reported as intermediates in the synthesis of tetraamines,[25,26] but only **III** has been used previously as a ligand for Cu(II),[27,28] Rh(I)[29] and Ir(I).[29]

† Electronic supplementary information (ESI): NMR spectra. See http://www.rsc.org/suppdata/dt/b1/b107378h/

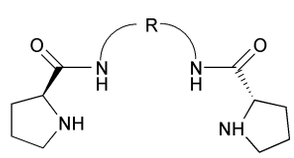

	R
III *S*,*S*-bprolenH_2	-CH_2CH_2-
IV *R*,*R*-(*S*,*S*)-bprolchxnH_2	*R*,*R*-1,2-cyclohexanediyl
V *S*,*S*-bprolbenH_2	1,2-benzenediyl

Fig. 2 Tetradentate diamide–dipyrrolidine ligands

Experimental

Reagents and solvents

Hydrogen (BOC Gases), 1,2-benzenediamine, activated carbon, HBr in acetic acid (BDH), palladium on activated carbon, *S*-proline (Aldrich), benzylchloroformate, 1,2-ethanediamine, $Ni(CH_3CO_2)_2{\cdot}4H_2O$, $NiCl_2{\cdot}6H_2O$ (Merck) triethylamine, NaOH (Ajax), *iso*-butylchloroformate (ICN Biomedicals), Na_2SO_4, acetone, methanol, ethanol, ethyl acetate, diethyl ether, and chloroform were of laboratory grade; argon (BOC Gases), toluene, acetonitrile (Ajax), Na_2CO_3 (Prolabo), $NaHCO_3$ (BDH) were AR grade; and were used as received in the preparation of the ligands and their nickel complexes. Ferrocene (Aldrich, 98%) was purified by sublimation prior to use in cyclic voltammetry.

The following compounds were prepared by known methods: *N*,*N*′-bis(2-pyridinecarboxamide)-1,2-ethane (bpenH_2) **I**,[13] and *N*,*N*′-bis(2-pyridinecarboxamide)-1,2-benzene (bpbH_2) **II**,[13] carbobenzoxy-*S*-proline,[30] *N*,*N*′-bis(carbobenzoxy-*S*-prolyl)-1,2-ethanediamine,[25] and *R*,*R*-1,2-cyclohexanediamine.[31]

Physical Measurements

Elemental microanalyses (C, H, and N) were performed at the Research School of Chemistry at the Australian National University or the University of Otago, New Zealand. Melting points were measured on a Gallenkamp melting point apparatus and are reported uncorrected. UV-Vis spectra of the

complexes in DMF (Ajax, HPLC grade) or methanol (APS Finechem, 99.8%) were recorded on a Hewlett Packard 8452A diode array spectrophotometer. FTIR spectra were recorded by diffuse reflectance infrared Fourier transform spectroscopy (KBr) on a Bio Rad FTS-40 spectrophotometer. ^{1}H NMR spectra were recorded at 25 °C on a Bruker AMX400 NMR spectrometer or a Bruker AC200 NMR spectrometer; in some experiments, a few drops of D_2O were added to identify labile protons. The ^{1}H-decoupled ^{13}C NMR spectra were recorded on a Bruker AC200 NMR spectrometer. Tetramethylsilane was used as the internal standard for the ^{1}H and ^{13}C spectra. Cyclic voltammetry was carried out using a BAS 100B Electrochemical Analyzer controlled by BAS 100W software. The complexes were dissolved in *N,N*-dimethylformamide (DMF) (Ajax, HPLC grade) or distilled water with 0.10 M tetra(*n*-butyl)ammonium perchlorate (TBAP) (Fluka, electrochemistry grade) or 0.10 M $NaClO_4$ (Aldrich, 99.99%), respectively, as the supporting electrolytes. A three-electrode system with a glassy-carbon working electrode, a Ag/AgCl reference electrode and a Pt wire auxiliary electrode was used. Full *iR* compensation was applied for all scans. The ferrocenium/ferrocene ($Fc^{+/0}$) couple was used as an internal redox potential standard for the DMF solutions.

Syntheses

***N,N′*-Bis(*S*-prolyl)-1,2-ethanediamine (*S,S*-bprolenH$_2$) III.** The synthesis was carried out by a modification of the method of Jun and Liu.[25] Palladium on activated carbon (~1 g, 10%) was added to *N,N′*-bis(carbobenzoxy-*S*-prolyl)-1,2-ethanediamine (34.6 g) in methanol (450 mL). Hydrogen was gently bubbled through the mixture until CO_2 production ceased (~90 h). The mixture was filtered through a Celite pad and the residue was washed with methanol (~100 mL). The combined filtrate and washings were filtered through a filter paper and the solvent was removed on a rotary evaporator. Ethanol (~100 mL) was added and evaporated to remove any residual water as an azeotrope. The product, a yellow coloured oil, was stored under nitrogen in the refrigerator for 5 d, during which time most of it solidified forming white crystals. The product was recrystallised from methanol/ethyl acetate as the hemihydrate, (7.40 g, 42%); mp 105–108 °C (lit.,[29] 92–93 °C) (Found: C, 54.84; H, 8.39; N, 21.02. $C_{12}H_{23}N_4O_{2.5}$ requires C, 54.73; H, 8.80; N, 21.28); ν_{max}/cm^{-1} 3306vs (amide NH), 2965s (CH), 2943s (CH), 2921w (CH), 2860s (CH), 2825w (CH), 1652vs (amide I), 1541vs (amide II), 1444s, 1311s (amide III), 1255s, 1235s, 1110s, 910s, 692s (amide V), (DRIFTS in KBr) (lit.,[29] 3278, 1646, 1552 cm^{-1}); δ_H(400 MHz, $CDCl_3$) 1.72 (4 H, m, pyrrolidine H_4), 1.90 (2 H, m, pyrrolidine H_3), 2.14 (2 H, m, pyrrolidine $H_{3'}$), 2.72 (2 H, br s, amine), 2.97 (4 H, m, pyrrolidine H_5), 3.37 (4 H, t, ethene bridge CH_2), 3.76 (2 H, dd, pyrrolidine H_2), 7.95 (2 H, br s, amide) (lit.,[29] 1.63–1.72 (4 H), 1.82–1.94 (2 H), 2.02–2.16 (2 H), 2.3–2.6 (2 H), 2.88 (2 H), 2.97 (2 H), 3.34–3.36 (4 H), 3.67 (2 H), 7.63–7.81 (2 H)); δ_C(200 MHz, $CDCl_3$) 26.1 (pyrrolidine C_4), 30.7 (pyrrolidine C_3), 39.1 (ethene bridge CH_2), 47.2 (pyrrolidine C_5), 60.5 (pyrrolidine C_2), 175.8 (*C*O) (lit.,[29] 25.96, 30.56, 39.05, 47.05, 60.61, 175.81).

***N,N′*-Bis(carbobenzoxy-*S*-prolyl)-*R,R*-1,2-cyclohexanediamine.** A modification of the method of Jun and Liu[26] was used to synthesise *N,N′*-bis(carbobenzoxy-*S*-prolyl)-*R,R*-1,2-cyclohexanediamine. Carbobenzoxy-*S*-proline (33.17 g) was dissolved in toluene (300 mL) and triethylamine (19.5 mL) was added. The solution was chilled to −5 °C in an ice/acetone bath and *iso*-butylchloroformate (17.3 mL) was added, followed by toluene (50 mL). The solution was stirred for 1 h. A cold solution of *R,R*-1,2-cyclohexanediamine (7.59 g) and triethylamine (19.5 mL) in chloroform (200 mL) was added. The flask was sealed with a $CaCl_2$ drying tube, and left stirring overnight at room temperature. The reaction mixture was filtered at the pump and the residue was washed with chloroform (50 mL). The combined filtrate and washings were extracted with water (200 mL), $NaHCO_3$ solution (200 mL, 3%), and water (200 mL). The organic layer was dried over anhydrous Na_2SO_4 and filtered. The solvent from the filtrate was removed on a rotary evaporator to give a white solid, which was recrystallised from acetone/diethyl ether, (26.37 g, 69%); δ_H(200 MHz, $CDCl_3$) 0.7–1.3 (4 H, m), 1.4–2.3 (12 H, m), 3.50 (6 H, m), 4.25 (2 H, t, pyrrolidine H_2), 5.18 (4 H, t, C_6H_5–CH_2), 6.3 (1 H, br s, amide), 6.7 (1 H, br s, amide), 7.35 (10 H, s, C_6H_5–CH_2).

***N,N′*-Bis(*S*-prolyl)-*R,R*-1,2-cyclohexanediamine (*R,R*-(*S,S*)-bprolchxnH$_2$) IV.** The carbobenzoxy protecting groups were removed by the method used for **III**. The product, a white solid, was dried over silica gel, (14.27 g, 101%); mp 179–181 °C (Found: C, 62.10; H, 8.88; N, 17.95. $C_{16}H_{28}N_4O_2$ requires C, 62.30; H, 9.15; N, 18.17%); ν_{max}/cm^{-1} 3315vs (amide NH), 3248w, 2972w (CH), 2935s (CH), 2860s (CH), 1637vs (amide I), 1523vs (amide II), 1510vs, 1456w, 1297w (amide III), 1110w, 880w, 695w (amide V), (DRIFTS in KBr); δ_H(400 MHz, $CDCl_3$) 1.25 (2 H, m, cyclohexane H_3 and H_6), 1.31 (2 H, m, cyclohexane H_4 and H_5), 1.66 (4 H, m, pyrrolidine H_4), 1.73 (2 H, m, cyclohexane $H_{4'}$ and $H_{5'}$), 1.77 (2 H, m, pyrrolidine H_3), 1.92 (2 H, br s, amine), 2.01 (2 H, m, cyclohexane $H_{3'}$ and $H_{6'}$), 2.11 (2 H, m, pyrrolidine $H_{3'}$), 2.92 (4 H, m, pyrrolidine H_5), 3.62 (2 H, m, cyclohexane H_1 and H_2), 3.66 (2 H, dd, pyrrolidine H_2), 7.59 (2 H, br s, amide); δ_C(200 MHz, $CDCl_3$) 24.8 (cyclohexane C_4 and C_5), 26.3 (pyrrolidine C_4), 30.8 (pyrrolidine C_3), 32.7 (cyclohexane C_3 and C_6), 47.2 (pyrrolidine C_5), 52.5 (cyclohexane C_1 and C_2), 60.6 (pyrrolidine C_2), 175.3 (CO).

***N,N′*-Bis(carbobenzoxy-*S*-prolyl)-1,2-benzenediamine.** Carbobenzoxy-*S*-proline (48.48 g) was dissolved in toluene (400 mL) and triethylamine (28.5 mL) was added. The solution was chilled to −10 °C in an ice/acetone bath and *iso*-butylchloroformate (25.5 mL) was added, followed by toluene (125 mL). The solution was stirred for 1 h. A cold solution of 1,2-benzenediamine (10.43 g) and triethylamine (28.5 mL) in chloroform (300 mL) was added. The flask was sealed with a $CaCl_2$ drying tube and left stirring overnight at room temperature. The reaction mixture was filtered at the pump and the residue was washed with toluene (~50 mL). The combined filtrate and washings were extracted with water (400 mL), $NaHCO_3$ solution (400 mL, 3%), and water (400 mL). The organic layer was dried over anhydrous Na_2SO_4 (~5 g) and filtered. The solvent from the filtrate was removed on a rotary evaporator, giving a very viscous brown coloured oil that solidified on cooling. The product was dissolved in boiling ethanol (500 mL) and activated carbon (14.5 g) was added. The mixture was boiled for 30 min and the hot solution was filtered. The filtrate was evaporated to dryness to give a pale brown coloured solid, (46.92 g, 85%); δ_H(200 MHz, $CDCl_3$) 1.8–2.4 (8 H, m, pyrrolidine), 3.52 (4 H, m, pyrrolidine), 4.49 (2 H, m, pyrrolidine H_2), 5.16 (4 H, m, C_6H_5–CH_2), 7.34 (14 H, m, benzene rings), 7.64 (1 H, br d, amide), 8.91 (1 H, br d, amide).

Synthesis of *N,N′*-bis(*S*-prolyl)-1,2-benzenediamine (*S,S*-bprolbenH$_2$) V. A solution of HBr in acetic acid (130 mL, 45%) was added to *N,N′*-bis(carbobenzoxy-*S*-prolyl)-1,2-benzenediamine (46.53 g). The mixture was heated for $2\frac{1}{4}$ h on a steam bath then left to cool. The reaction mixture was filtered and the solvent was removed from the filtrate on a rotary evaporator. Diethyl ether was added to the residue, which was triturated and left to stand; the supernatant was discarded. The residue was dissolved by shaking with NaOH solution (200 mL, 1 M; 50 mL, 10 M) and chloroform (200 mL). The aqueous layer was extracted with chloroform (4 × 100 mL). The combined organic layers were dried over anhydrous Na_2SO_4 (~10 g), filtered and the solvent was removed on a rotary evaporator. The product

was recrystallised from chloroform/diethyl ether. This gave a pale brown coloured powder (7.14 g, 29%); ν_{max}/cm^{-1} 3312s (amide NH), 3254s, 2969s (CH), 2946w (CH), 2915w (CH), 1665vs (amide I), 1594s, 1528vs (amide II), 1473s, 1301s (amide III), 1104s, 906w, 869s, 771s, (DRIFTS in KBr); δ_H(400 MHz, $CDCl_3$) 1.72 (6 H, m, pyrrolidine H_4 and amine), 2.00 (2 H, m, pyrrolidine H_3), 2.15 (2 H, m, pyrrolidine $H_{3'}$), 2.96 (4 H, m, pyrrolidine H_5), 3.84 (2 H, dd, pyrrolidine H_2), 7.09 (2 H, m, benzene H_4 and H_5), 7.62 (2 H, m, benzene H_3 and H_6), 9.64 (2 H, br s, amide); δ_C(200 MHz, $CDCl_3$) 26.3 (pyrrolidine C_4), 30.9 (pyrrolidine C_3), 47.4 (pyrrolidine C_5), 61.1 (pyrrolidine C_2), 124.0 (benzene C_3 and C_6), 125.7 (benzene C_4 and C_5), 129.8 (benzene C_1 and C_2), 174.2 (CO). The crude product was used in the synthesis of the nickel complex but a small sample was purified for microanalysis. A methanol solution of the crude product was loaded onto a silica column (11 × 2 cm, silica gel 60, 35–70 mesh) and a yellow band was eluted with methanol, which was discarded. The fraction that was eluted with methanol after the yellow band and a subsequent fraction eluted with dichloromethane contained pure *S*,*S*-bprolbenH_2. The solvent was removed from these fractions on a rotary evaporator and the residues were combined. The white powder contained 0.75 CH_3OH of crystallisation (Found: C, 62.34; H, 7.26; N, 16.69. $C_{16.75}H_{25}N_4O_{2.75}$ requires C, 61.64; H, 7.72; N, 17.16%), mp 154–159 °C.

[Ni^{II}(bprolenH_{-4})]·H_2O 1. *Method 1.* Nickel(II) acetate tetrahydrate (0.196 g) was dissolved in water (15 mL) and **III** (0.200 g) was added. The green-coloured solution was heated on a steam bath then allowed to evaporate slowly. The non-crystalline residue thus formed was dissolved in water (~5 mL), further heated, and NaOH solution (1 M) was added dropwise until the colour of the solution changed to orange. The solution was filtered and the filtrate was left to evaporate slowly. Small yellow needle-like crystals formed over several days and were collected at the pump and dried under reduced pressure over silica gel. The product was recrystallised from methanol (7.3 mg, 3%) (Found: C, 44.39; H, 5.53; N, 17.01. $C_{12}H_{18}N_4O_3Ni$ requires C, 44.34; H, 5.58; N, 17.24); ν_{max}/cm^{-1} 3479s, 2940s (CH), 2847s (CH), 1627vs (amide I), 1612vs (imine C=N), 1411s (amide C–N), 1328s, 1032s, 508s, (DRIFTS in KBr); δ_H(400 MHz, CD_3OD) 2.09 (4 H, quintet, 7.6Hz, 8.0 Hz, pyrroline H_4), 2.71 (4 H, tt, 2.4 Hz, 8.0 Hz, pyrroline H_3), 3.24 (4 H, s, ethene bridge CH_2), 3.76 (4 H, tt, 2.4 Hz, 7.6 Hz, pyrroline H_5).

Method 2. Nickel(II) acetate tetrahydrate (0.196 g) was dissolved in water (10 mL) and a solution of **III** (0.208 g) in water (10 mL) was added. The pH value was raised to ~8 by the addition of $NaHCO_3$ solution (10 mL, 1 M) and a fine precipitate started to form. Sodium carbonate (20 mL, 1 M) was added to raise the pH value to ~10, and this resulted in the precipitation of a large amount of fine solid. The mixture was heated on a steam bath for an hour, during which most of the solid dissolved and the colour changed from green–yellow to bright yellow. The mixture was filtered and the pH value of the filtrate was ~10. Slow evaporation of the filtrate gave tiny needle-like yellow-coloured crystals, which were collected at the pump, washed with ice-cold water (2 × 2 mL), and dried over silica gel. A second crop was obtained from the filtrate and purified by recrystallisation from methanol, (0.055 g, 22%); λ_{max}/nm (CH_3OH) 242 (sh, ε/dm^3 mol^{-1} cm^{-1}, 6.8 × 10^3), 382 (8.3 × 10^3), 424 (sh, 3.3 × 10^3); δ_H(200 MHz, CD_3OD) 2.09 (4 H, quintet); 2.71 (4 H, tt); 3.24 (4 H, s); 3.76 (4 H, tt); δ_C(200 MHz, dmso-d_6) 20.3 (pyrroline C_4), 32.7 (pyrroline C_3), 48.0 (pyrroline C_5), 57.9 (ethene bridge CH_2), 164.6 (pyrroline C_2), 177.4 (CO).

[Ni^{II}(*S*,*S*-bprolen)]·H_2O 2. The syntheses were carried out using Schlenk techniques under an argon atmosphere. All solvents and prepared solutions were degassed thoroughly before use by repeated evacuation followed by purging with argon.

Method 1. Nickel(II) acetate tetrahydrate (0.196 g) was dissolved in water (10 mL) and a solution of **III** (0.203 g) in water (10 mL) was added. A NaOH solution (3 mL, 0.4 M) was added and the solutions were mixed thoroughly. The water was evaporated under reduced pressure, and the residue was dissolved in methanol (30 mL) and filtered. The filtrate was evaporated under reduced pressure, and the residue was dissolved in methanol (20 mL) and filtered. Methanol was added to the filtrate to increase the volume to ~40 mL and acetonitrile (15 mL) was added. Slow evaporation of the methanol/acetonitrile solution over a period of several days under argon did not produce crystals, so diethyl ether (15 mL) was added and the mixture was allowed to stand for a further 2 d. The supernatant was decanted, leaving orange-coloured crystals that were washed with methanol/acetonitrile in a 1 : 5 ratio (12 mL) and dried under reduced pressure to give a yellow-coloured powder, (0.055 g, 21%) (Found: C, 43.25; H, 6.49; N, 16.76. $C_{22}H_{22}N_4O_3Ni$ requires C, 43.67; H, 6.71; N, 16.98%); ν_{max}/cm^{-1} 3092s, 2955s (CH), 2881s (CH), 2867s (CH), 1599vs (amide I), 1449w 1425s (amide C–N), 1317w, 1222w, 1071w, 1051w, 1005w, 934s, 765w (DRIFTS in KBr); δ_H(400 MHz, dmso-d_6) 1.54 (2 H, m, pyrrolidine H_4), 1.66 (2 H, m, pyrrolidine H_3), 1.80 (2 H, m, pyrrolidine $H_{3'}$), 1.95 (2 H, m, pyrrolidine $H_{4'}$), 2.67 (2 H, m, pyrrolidine H_5), 2.76 (4 H, s, ethene bridge CH_2), 3.14 (2 H, m, pyrrolidine $H_{5'}$), 3.3 (2 H, m, pyrrolidine H_2), 4.37 (2H, q, amine); δ_C(400 MHz, dmso-d_6) 25.5 (pyrrolidine C_4), 29.3 (pyrrolidine C_3), 47.0 (ethene bridge CH_2), 49.0 (pyrrolidine C_5), 66.2 (pyrrolidine C_2), 177.1 (CO).

Method 2. Nickel(II) chloride hexahydrate (0.279 g) was dissolved in water (10 mL) and a solution of **III** (0.311 g) in water (10 mL) was added. A NaOH solution (10 mL, 1 M) was added and the solutions were mixed thoroughly. The water was evaporated under reduced pressure, the residue was dissolved in methanol (25 mL), and the solution was filtered. The filtrate was evaporated under reduced pressure, the residue was dissolved in methanol (20 mL) and the solution was filtered. The filtrate was evaporated under reduced pressure and the residue was removed from the Ar atmosphere. The remainder of the synthesis was carried out in air. The residue was dissolved in methanol (15 mL) and loaded onto a LH20 lipophilic Sephadex column (2.5 × 14 cm) and the complexes were eluted with methanol. A major fast moving yellow band and a minor, slower moving light orange band were eluted. The faster moving yellow band was collected and slowly evaporated to dryness. The residue was recrystallised from methanol yielding light orange crystals, (0.188 g, 49%); λ_{max}/nm (CH_3OH) 252 (sh, ε/dm^3 mol^{-1} cm^{-1} 7.9 × 10^3), 380 (3.9 × 10^2); δ_H(200 MHz, dmso-d_6) 1.5–1.8 (4 H, m), 1.8–2.1 (4 H, m), 2.69 (2 H, m), 2.75 (4 H, s), 3.14 (2 H, m), 3.3 (2 H, m), 4.40 (2 H, q).

[Ni^{II}(*R*,*R*-(*S*,*S*)-bprolchxn)]·$\frac{5}{2}H_2O$ 3. Nickel(II) acetate tetrahydrate (0.203 g) was dissolved in water (10 mL) by heating on a steam bath and a solution of **IV** (0.252 g) in water (10 mL) was added. Sodium hydroxide solution (3 mL, 1 M) was added, which changed the colour of the reaction solution from green to yellow. The solution was filtered, and the filtrate was left to evaporate slowly. Orange crystals formed in the filtrate and were collected at the pump, washed with water (2 × ~5 mL), and dried under reduced pressure. A second crop of crystals was obtained from the filtrate and washings. The product was recrystallised from methanol (0.165 g, 50%) (Found: C, 47.14; H, 7.60; N, 13.42. $C_{16}H_{31}N_4O_{4.5}Ni$ requires C, 46.86; H, 7.62; N, 13.66%); λ_{max}/nm (CH_3OH) 238 (ε/dm^3 mol^{-1} cm^{-1} 1.4 × 10^4), 418 (2.3 × 10^2); ν_{max}/cm^{-1} 3439w, 3364w, 3106s, 2981w (CH), 2971w (CH), 2934s (CH), 2903w (CH), 2870s (CH), 2855w (CH), 2839w (CH), 1611s, 1575vs (amide I), 1444s, 1417s (amide C–N), 1343s, 1297w, 1238w, 932s (DRIFTS in KBr); δ_H(400 MHz, dmso-d_6) 0.88 (2 H, m, cyclohexane H_3 and H_6), 1.03 (2 H, m, cyclohexane H_4 and H_5), 1.41 (2H, m,

Table 1 Summary of crystal data and details of structure refinements for **1**, **2**, **3** and **4**

Compound	**1**·H_2O	**2**·H_2O	**3**·3H_2O	**4**·D_2O·CD_3OD
Model formula	$C_{12}H_{18}N_4NiO_3$	$C_{12}H_{20}N_4NiO_3$	$C_{16}H_{32}N_4NiO_5$	$C_{17}H_{26}N_4NiO_4$
M_w	325.00	327.03	419.17	409.13
Crystal system	Triclinic	Trigonal	Orthorhombic	Orthorhombic
Space group (no.)	$P\bar{1}$ (2)	$P3_221$ (154)	$P2_12_12_1$ (19)	$P2_12_12_1$ (19)
a/Å	9.748(1)	8.5856(14)	9.0175(3)	11.760(2)
b/Å	9.923(1)	8.5856	10.1232(3)	18.409(3)
c/Å	8.383(1)	17.3694(18)	21.1448(7)	8.571(2)
α/°	105.53(1)	—	—	—
β/°	104.40(1)	—	—	—
γ/°	112.37(1)	120.00	—	—
V/Å^3	664.2(2)	1108.8(2)	1930.22(11)	1855.6(6)
Z	2	3	4	4
T/°C	21	21	20	21
μ/mm^{-1}	2.245 (Cu-Kα)	2.017 (Cu-Kα)	1.039 (Mo-Kα)	1.770 (Cu-Kα)
N	2250	1514	20641	1931
N_{obs}	1911 ($I > 3\sigma(I)$)	1266 ($I > 2\sigma(I)$)	4221 ($I > 2\sigma(I)$)	1808 ($I > 2\sigma(I)$)
R	0.051	0.0389	0.0303	0.0339
R_w	0.060	0.1093	0.0795	0.0967

cyclohexane $H_{4'}$ and $H_{5'}$), 1.51 (2 H, m, pyrrolidine H_4), 1.69 (2 H, m, pyrrolidine H_3), 1.76 (2 H, m, pyrrolidine $H_{3'}$), 1.88 (2 H, m, pyrrolidine $H_{4'}$), 2.62 (2 H, m, pyrrolidine H_5), 2.66 (2 H, m, cyclohexane H_1 and H_2), 2.82 (2 H, m, cyclohexane $H_{3'}$ and $H_{6'}$), 3.06 (2 H, m, pyrrolidine $H_{5'}$), 3.38 (2 H, q, pyrrolidine H_2), 4.17 (2 H, q, amine); δ_C(200 MHz, dmso-d_6) 25.2 (cyclohexane C_4 and C_5 or pyrrolidine C_4), 25.4 (pyrrolidine C_4 or cyclohexane C_4 and C_5), 28.8 (pyrrolidine C_3), 31.6 (cyclohexane C_3 and C_6), 49.0 (pyrrolidine C_5), 65.8 (pyrrolidine C_2), 68.6 (cyclohexane C_1 and C_2), 177.9 (CO).

[Ni^{II}(*S*,*S*-bprolben)]·2H_2O 4. Nickel(II) acetate tetrahydrate (0.167 g) was dissolved in water (10 mL) by heating on a steam bath. A solution of **V** (0.204 g) in methanol (10 mL) was added to the hot Ni(II) acetate solution. The colour of the solution changed immediately from green to orange. The product crystallised as the solution cooled, and was collected at the pump after the mixture had stood for 2 d. The dark yellow, crystalline product was washed with ice-cold water (5 mL), air dried, then dried under reduced pressure over silica gel, (0.182 g, 69%); (Found: C, 49.11; H, 5.23; N, 14.45. $C_{16}H_{24}N_4O_4Ni$ requires C, 48.63; H, 6.12; N, 14.18%); λ_{max}/nm (CH_3OH) 216 (ε/dm^3 mol^{-1} cm^{-1} 3.1 × 10^4), 244 (sh, 1.3 × 10^4), 274 (1.5 × 10^4), 294 (1.7 × 10^4), 416 (2.1 × 10^2); ν_{max}/cm^{-1} 3456w, 3248w, 3117w, 2972w (CH), 2872w (CH), 1605vs (amide I), 1569vs (aromatic ring skeletal vibration), 1481s, 1454s, 1403s, 1033w, 755s (CH deformation) (DRIFTS in KBr); δ_H(400 MHz, CD_3OD) 1.75 (2 H, m, pyrrolidine H_4), 1.96 (2 H, m, pyrrolidine $H_{4'}$), 2.15 (4 H, m, pyrrolidine H_3), 2.89 (2 H, m, pyrrolidine H_5), 3.45 (2 H, m, pyrrolidine $H_{5'}$), 3.72 (2 H, q, pyrrolidine H_2), 4.51 (2 H, q, amine), 6.71 (2 H, dd, benzene H_4 and H_5), 8.08 (2 H, dd, benzene H_3 and H_6); δ_C(200 MHz, dmso-d_6) 25.6 (pyrrolidine C_4), 29.8 (pyrrolidine C_3), 49.4 (pyrrolidine C_5), 66.8 (pyrrolidine C_2), 118.6 (benzene C_3 and C_6), 120.3 (benzene C_4 and C_5), 142.9 (benzene C_1 and C_2), 177.0 (CO).

[Ni^{II}(bpen)] 5. The complex was prepared by the published method[17] and recrystallised from methanol (82%); λ_{max}/nm (CH_3OH) 256 (ε/dm^3 mol^{-1} cm^{-1} 1.5 × 10^4), 382 (7.4 × 10^3); ν_{max}/cm^{-1} 1633vs (amide I), 1604vs, 1418m (amide III), 755m, 685m (DRIFTS in KBr) (lit.,[17] 1630 and 1420 cm^{-1}).

[Ni^{II}(bpb)] 6. The complex was prepared by the published method[15] and recrystallised from DMF (97%); λ_{max}/nm (DMF) 324 (ε/dm^3 mol^{-1} cm^{-1} 1.9 × 10^4), 372 (sh, 8.1 × 10^3), 446 (sh, 3.1 × 10^3); ν_{max}/cm^{-1} 1639vs (amide I), 1604vs, 1576m, 1485m, 1398m, 745vs, 680m (DRIFTS in KBr) (lit.,[15] 1640, 1605, 1570, 1485, 1390, 750, 680 cm^{-1}).

X-Ray crystallography

Summaries of the data collection and solutions and refinements for **1**, **2**, **3** and **4** are given in Table 1.

Data for **1**·H_2O, **2**·H_2O and **4**·D_2O·CD_3OD were collected on a Rigaku AFC7R diffractometer employing graphite-monochromated Cu-Kα radiation from a rotating anode generator. Data for **3**·H_2O were collected on a Bruker SMART 1000 diffractometer with graphite-monochromated Mo-Kα generated from a sealed tube. In general, crystal data processing and calculations were undertaken with the TEXSAN[32–37] interface. The data integration and reduction for **3**·H_2O were undertaken with SAINT and XPREP.[38] All data were corrected for Lorentz and polarisation effects. An empirical absorption correction based on azimuthal scans of three reflections was applied to the data for **1**·H_2O and **2**·H_2O and a correction determined from equivalent reflections with SADABS[39] was applied to the data for **3**·H_2O. An analytical correction was applied to that data for **4**·D_2O·CD_3OD. Non-hydrogen atoms were modelled with anisotropic thermal parameters and in general the hydrogen atoms were included in the refinement at calculated positions with group thermal parameters.

1·H_2O. Slow evaporation of a methanol solution produced red prismatic crystals of suitable quality for X-ray diffraction studies. The structure was solved in the space group $P\bar{1}$ (no. 2) by heavy-atom Patterson methods[40] and expanded using Fourier techniques.[41] The asymmetic unit includes a water molecule and the water hydrogens were located and refined with isotropic thermal parameters.

2·H_2O. A yellow prismatic fragment cut from a twinned crystal grown from methanol was used for the structure determination. The structure was solved in the space group $P3_221$ (no. 154) by direct methods with SHELXS-97,[42] and extended and refined with SHELXL-97.[43]

The complex straddles a two-fold axis passing through the metal centre. The asymmetric unit contains a water molecule (also located on a two-fold axis), and no hydrogens were included in the model for the water molecule. The Flack parameter[44–46] refined to 0.00(5).

3·3H_2O. Slow evaporation of a methanol/acetonitrile solution of the product produced orange–yellow prismatic crystals suitable for X-ray crystallography. The structure was solved in the space group $P2_12_12_1$ (no. 19) by direct methods with SIR97,[47] and extended and refined with SHELXL-97.[43] The hydrogen sites of the water solvate molecules were located and refined; the O(5) hydrogen bond lengths were restrained. The

absolute structure was established with the Flack parameter[44,45] refining to 0.00(1).

4·D_2O·CD_3OD. A CD_3OD solution of the complex prepared for NMR spectroscopy with three drops of D_2O added was left standing in a sealed NMR tube for 2 weeks, and yellow columnar-like crystals suitable for X-ray crystallography formed during this time. The structure was solved in the space group $P2_12_12_1$(no. 19) by direct methods with SIR97,[47] and extended and refined with SHELXL-97[43] using the XSHELL interface.[48] The two water hydrogens were located and modelled with isotropic thermal parameters. The absolute structure was established with the Flack parameter[44,45] refining to 0.01(5).

CCDC reference numbers 169589–169592.

See http://www.rsc.org/suppdata/dt/b1/b107378h/ for crystallographic data in CIF or other electronic format.

Results and discussion

Ligand syntheses

The ligands **III**, **IV** and **V** were synthesised from *S*-proline (Scheme 1). The published procedure[26] for the synthesis of *N,N′*-bis(carbobenzoxy-*S*-prolyl)-*R*,*R*-1,2-cyclohexanediamine only used a 1.16 : 1.00 mole ratio of CBZ-S-proline: *R*,*R*-1,2-cyclohexanediamine, but use of the correct 2.00 : 1.00 ratio increased the yield from 47 to 69%. The removal of the carbobenzoxy protecting groups with HBr in acetic acid was considerably faster than the use of H_2 over a Pd/C catalyst, but the latter method produced greater yields with a higher degree of purity. The yield of crude **IV** was ~100% and elemental analyses and NMR spectra showed that it was of sufficient purity that recrystallisation was not required to make the complex. The mp of **III** was 13 °C higher than the reported value[29] indicating that it was of higher purity. The amide NH stretch also occurred at a higher frequency (possibly due to the inclusion of $0.5H_2O$ altering the amide hydrogen-bonding), and the ^1H and ^{13}C NMR data for **III** were in good agreement with the literature values.[27,29] The ^1H NMR signals of **IV** and **V** were assigned from the ^1H COSY NMR spectra (Figs. S2 and S3, Supporting Information †). The ^1H NMR resonances from the cyclohexane and pyrrolidine rings of **IV** overlapped in the 1D spectrum but were easily distinguished in the COSY spectrum as there were no cross-peaks between the two ring systems. The IR bands were assigned according to Bellamy[49] and by comparison to the IR spectra of **I**[17] and **II**.[15] The most prominent features of the IR spectra were the amide NH stretch, the amide I and amide II bands. This is the first report of the isolation of the chiral ligands **IV** and **V** in a pure form, along with their detailed characterisation. The synthetic scheme can be readily adapted to produce new ligands of this class by changing the diamine used as the central bridging group, and has many potential applications in the production of chiral tetradentate ligands. Complexes with these ligands have the potential to be used in chiral resolutions,[50] catalysis[29,51] and selective DNA damage.[2,3,5,7,8,10]

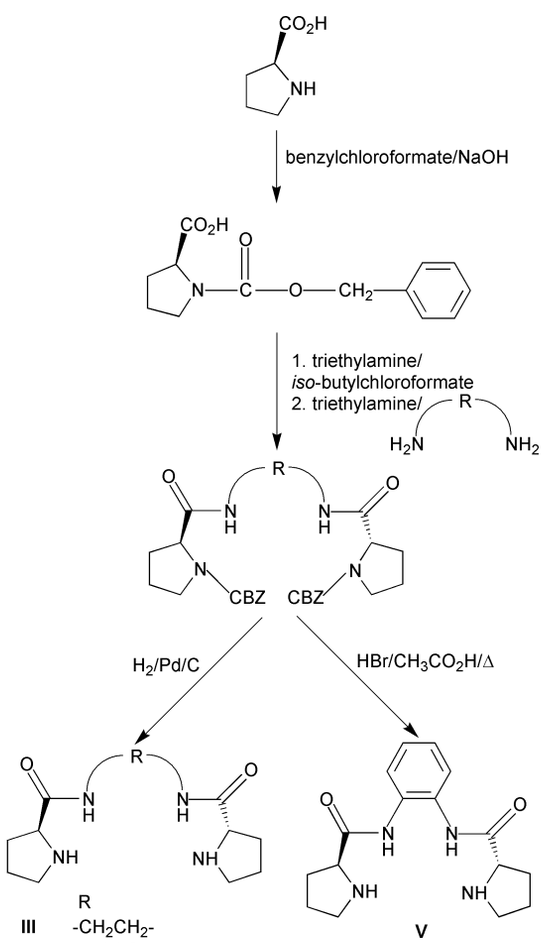

Scheme 1 Synthesis of tetradentate diamide-dipyrrolidine ligands

Nickel complexes

Nickel(II) complexes with **III** and **IV** were prepared by the addition of base to deprotonate the ligand amides. The complex with **V** was prepared directly by mixing, since the acetate counter ion was sufficiently basic to deprotonate the amide groups. The absence of the amide NH stretching and amide II bands from the IR spectra of the Ni complexes showed that the amide groups were deprotonated. The amide I bands occurred at lower frequencies in the complexes than in the free ligands, which was consistent with coordination of the ligand *via* amide nitrogen atoms.

Two different complexes, **1** and **2**, were obtained from the reaction of **III** with Ni(II), depending on the conditions under which the reaction took place (Scheme 2). The reaction of Ni(II) and **III** in air in the presence of base (OH^- or CO_3^{2-}), produced a Ni(II) complex where the two amine groups of the pyrrolidine rings were oxidised to imines, forming 1-pyrroline rings. When CO_3^{2-} was used (method 2) a large amount of precipitate, that was presumed to be $NiCO_3$, formed. The precipitate gradually dissolved as the ligand coordinated, forming a soluble yellow complex. The $Ni(CH_3CO_2)_2$/**III** reaction under Ar, produced **2** in which the ligand was not oxidised. Once isolated, the product could be handled in air as a solid without significant decomposition or ligand oxidation. The methanol solution of **2** is also air-stable, *e.g.*, a CD_3OD solution that was exposed to the air for a month revealed no **1** or other decomposition products by ^1H NMR spectroscopy. This allowed the purification of crude

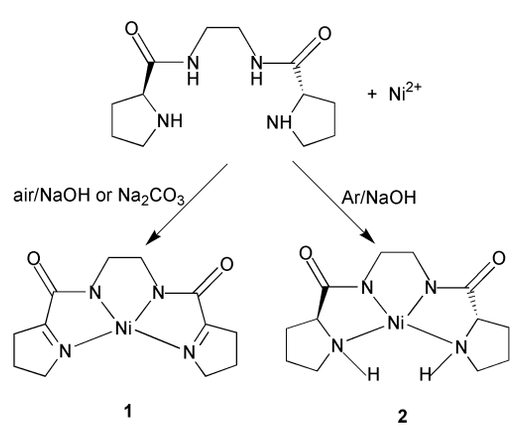

Scheme 2 Synthesis of nickel(II) complexes with **III**

Table 2 Selected bond distances (Å) and angles (°) of **1** involving the non-hydrogen atoms

Ni1–N1	1.893(3)	N1–C4	1.281(5)
Ni1–N2	1.835(3)	N2–C5	1.325(5)
Ni1–N3	1.827(3)	N2–C6	1.461(4)
Ni1–N4	1.898(3)	N3–C7	1.470(5)
O1–C5	1.243(5)	N3–C8	1.316(5)
O2–C8	1.230(5)	N4–C9	1.285(5)
N1–C1	1.478(4)	N4–C12	1.466(5)
N1–Ni1–N2	84.5(1)	Ni1–N2–C6	117.7(3)
N1–Ni1–N3	169.1(1)	C5–N2–C6	123.6(3)
N1–Ni1–N4	106.5(1)	Ni1–N3–C7	116.7(3)
N2–Ni1–N3	84.7(1)	Ni1–N3–C8	118.8(3)
N2–Ni1–N4	168.5(1)	C7–N3–C8	124.2(3)
N3–Ni1–N4	84.3(1)	Ni1–N4–C9	112.6(2)
Ni1–N1–C1	136.3(3)	Ni1–N4–C12	136.5(3)
Ni1–N1–C4	113.2(3)	C9–N4–C12	110.7(3)
C1–N1–C4	110.4(3)	O1–C5–N2	129.0(4)
Ni1–N2–C5	116.7(2)	O2–C8–N3	129.3(4)

product in method 2 in air using column chromatography, which greatly improved the yield. The crystal used to determine the structure by X-ray diffraction was obtained by slow evaporation under air of a methanol solution.

X-Ray crystallography

The most significant features of the crystal structure of **1**·H_2O (Fig. 3) are the N1–C4 and N4–C9 double bond lengths

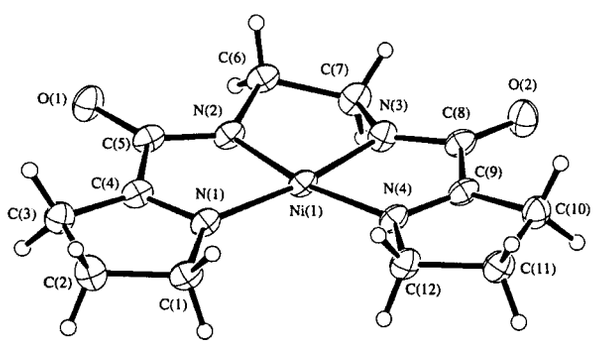

Fig. 3 ORTEP[52] depiction of **1** with 25% atom displacement ellipsoids

(Table 2) of 1.281(5) and 1.285(5) Å. The sp^2 hybridisation of N1 and N4 was also shown by their trigonal planar geometry. The 1-pyrroline rings are almost coplanar with the least-squares plane defined by the four nitrogen atoms, and the dihedral angles are 7.0(2) and 4.2(2)°. The angle between the two 1-pyrroline rings is 11.1(2)°.

The coordination geometry about the Ni in **1** is square-planar, with two Ni–N(amide) and two Ni–N(imine) bonds. The nickel atom deviates by just 0.033(1) Å from the least-squares plane defined by the four nitrogen atoms. The deviation of the nitrogens from the coordination least-squares planes ranges from 0.018(5) to 0.022(5) Å. The Ni–N(amide) bond lengths of 1.835(3) and 1.827(3) Å, are within the range (1.820–2.02 Å) reported for other deprotonated Ni–N(amide) bonds.[18,20,23,24,53–56] The Ni–N(imine) bond lengths of 1.893(3) and 1.898(3) Å are also typical (1.840–2.065 Å).[57–63]

The molecular structure of **2**·H_2O (Fig. 4) has a two-fold symmetry axis through the Ni atom. The non-hydrogen bond distances and angles are given in Table 3. The crystal structure showed that the amines in the pyrrolidine rings of the ligand were preserved during the formation of the complex. The N1–C4 bond length is 1.503(4) Å, and the geometries about N1 and C4 are tetrahedral. The amine nitrogen atoms are chiral and both have the *S* configuration. The Ni atom is coordinated to two deprotonated amide nitrogens and two amines in a square-planar geometry. The pyrrolidine rings of the ligand are non-planar and are at a 60.3(2)° angle to the coordination plane.

Table 3 Selected bond distances (Å) and angles (°) of **2** involving the non-hydrogen atoms

Ni1–N1	1.925(2)	Ni1–N2	1.822(2)
O1–C5	1.249(4)	N1–C1	1.498(4)
N1–C4	1.503(4)	N2–C5	1.314(4)
N2–C6	1.462(4)		
N1–Ni1–N1′	101.5(2)	C4–N1–Ni1	110.0(2)
N1–Ni1–N2	86.4(1)	C5–N2–C6	123.4(2)
N1–Ni1–N2′	171.4(1)	C5–N2–Ni1	119.3(2)
N2–Ni1–N2′	86.0(2)	C6–N2–Ni1	115.8(2)
C1–N1–C4	107.3(3)	O1–C5–N2	126.3(3)
C1–N1–Ni1	113.7(2)		

Symmetry operator: $y, x, 1 - z$

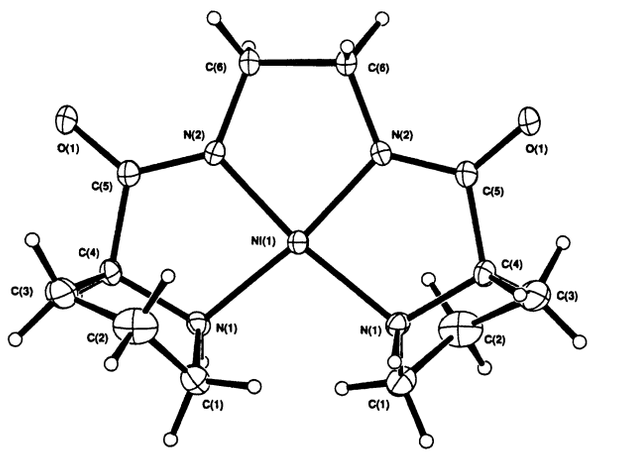

Fig. 4 ORTEP[52] representation of **2** with 25% atom displacement ellipsoids

The deprotonated Ni–N(amide) bond length of 1.822(2) Å is significantly shorter than the Ni–N(amine) bond length of 1.925(2) Å. The Ni–N(amide) bond length is slightly, but not significantly, shorter than the average value in **1**, but the Ni–N(amine) bond length is significantly longer than the Ni–N(imine) bonds in **1**. The coordination about the Ni atom is square-planar, and it lies within the plane defined by the four N atoms. The deviation of the nitrogens from the coordination least-squares planes ranges from 0.037(3) to 0.078(4) Å.

The ORTEP diagram of the complex in **3**·3H_2O is given in Fig. 5. The non-hydrogen bond distances and angles are in Table

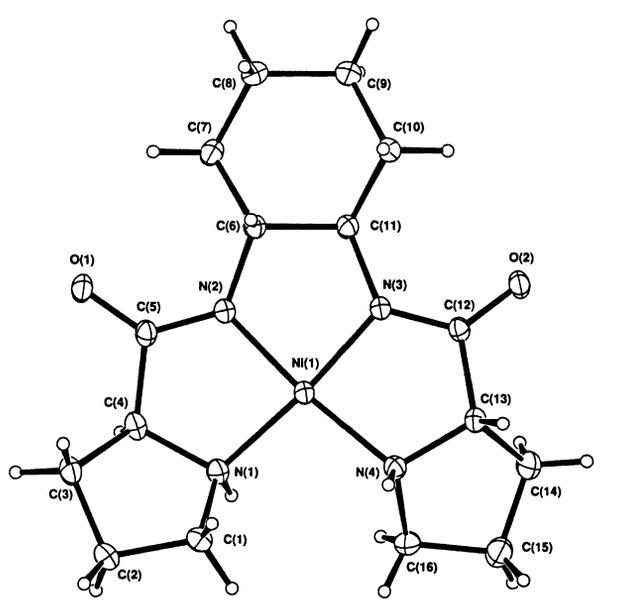

Fig. 5 ORTEP[52] representation of **3** with 25% atom displacement ellipsoids

Table 4 Selected bond distances (Å) and angles (°) of **3** involving the non-hydrogen atoms

Ni1–N3	1.839(2)	Ni1–N2	1.845(2)
Ni1–N1	1.921(2)	Ni1–N4	1.932(2)
O1–C5	1.259(3)	O2–C12	1.262(3)
N1–C1	1.486(3)	N1–C4	1.515(3)
N2–C5	1.314(3)	N2–C6	1.482(3)
N3–C12	1.320(3)	N3–C11	1.475(3)
N4–C16	1.507(3)	N4–C13	1.510(3)
N3–Ni1–N2	86.70(8)	C5–N2–Ni1	118.3(2)
N3–Ni1–N1	170.36(8)	C6–N2–Ni1	113.5(1)
N2–Ni1–N1	86.80(8)	C12–N3–C11	123.4(2)
N3–Ni1–N4	86.68(7)	C12–N3–Ni1	116.6(2)
N2–Ni1–N4	172.34(8)	C11–N3–Ni1	113.5(1)
N1–Ni1–N4	100.24(8)	C16–N4–C13	106.1(2)
C1–N1–C4	106.4(2)	C16–N4–Ni1	119.4(2)
C1–N1–Ni1	120.6(2)	C13–N4–Ni1	109.0(1)
C4–N1–Ni1	109.7(1)	O1–C5–N2	128.2(2)
C5–N2–C6	125.6(2)	O2–C12–N3	128.1(2)

4. The Ni atom is bound to two amines and two deprotonated amide nitrogens and has square-planar coordination geometry. The deviation of the nitrogens from the coordination least-squares planes ranges from 0.077(2) to 0.101(2) Å. The deviations of the N atoms from the coordination plane are slightly larger than those observed in the crystal structures of **1**, **2** and **4**; perhaps due to the central *trans*-cyclohexane bridge. The amine nitrogens are chiral and both have a *S* configuration. The Ni–N(amide) bond lengths are 1.839(2) Å and 1.845(2) Å, and are slightly longer than the 1.822(2) Å Ni–N(amide) bond length of **2**. The Ni–N(amine) bond lengths of 1.921(2) and 1.932(2) Å are not significantly different from the Ni—N(amine) bond length of 1.925(2) Å in **2**. The longer Ni–N(amide) bond lengths may be due to distortion caused by the central *trans*-cyclohexane bridge.

The ORTEP diagram of the Ni complex in **4**·D_2O·CD_3OD (Fig. 6) shows that the Ni atom is square-planar and coordinated to two amines and two deprotonated amide nitrogens. The Ni–N(amide) bond lengths (Table 5) of 1.833(3) Å and 1.842(3) Å are significantly shorter than the Ni–N(amine) bond lengths of 1.919(3) and 1.922(3) Å. The coordinated N atoms are co-planar, with deviations ranging from 0.018(4) to 0.022(4) Å. The dihedral angle between the benzene ring and the coordination plane is 1.0(1)°. The puckered pyrrolidine rings were not oxidised during the synthesis of the complex; the amine nitrogens are chiral and both have the *S* configuration.

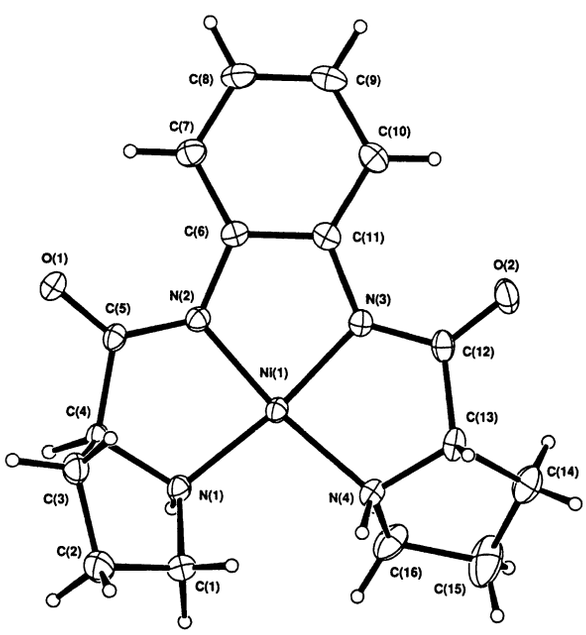

Fig. 6 ORTEP[52] representation of **4** with 25% atom displacement ellipsoids

Table 5 Selected bond distances (Å) and angles (°) of **4** involving the non-hydrogen atoms

Ni1–N2	1.833(3)	Ni1–N3	1.842(3)
Ni1–N1	1.919(3)	Ni1–N4	1.922(3)
O1–C5	1.243(4)	O2–C12	1.250(5)
O3–C17	1.375(7)	N1–C1	1.509(5)
N1–C4	1.512(4)	N2–C5	1.327(5)
N2–C6	1.416(4)	N3–C12	1.323(4)
N3–C11	1.415(5)	N4–C16	1.487(5)
N4–C13	1.499(5)		
N2–Ni1–N3	85.6(1)	C5–N2–Ni1	118.2(2)
N2–Ni1–N1	86.8(1)	C6–N2–Ni1	114.8(2)
N3–Ni1–N1	172.3(1)	C12–N3–C11	126.8(3)
N2–Ni1–N4	172.0(1)	C12–N3–Ni1	118.1(3)
N3–Ni1–N4	86.6(1)	C11–N3–Ni1	114.3(2)
N1–Ni1–N4	101.1(1)	C16–N4–C13	106.0(3)
C1–N1–C4	106.3(3)	C16–N4–Ni1	117.3(2)
C1–N1–Ni1	118.6(2)	C13–N4–Ni1	108.6(2)
C4–N1–Ni1	108.9(2)	O1–C5–N2	128.7(3)
C5–N2–C6	125.9(3)	O2–C12–N3	126.8(4)

In all four crystal structures, the bond angles formed by the chelate rings about the Ni are less than the ideal value of 90° for a square-planar complex, with the angle between the terminal nitrogen donors >100° to compensate. The uniform *S* configuration of the amine nitrogens in **2**, **3** and **4** shows that their chirality was determined by the fixed *S* configuration at position 2 of the pyrrolidine rings.

NMR spectra of nickel complexes

The ^{1}H NMR spectrum of **1** (Fig. S4, Supporting Information †) was much simpler than that of **III** (Figure S1, Supporting Information †). There were only four signals, and the individual proton–proton couplings were determined along with the coupling constants by selective decoupling experiments (Figs. S5–S7, Supporting Information †). The resonances at 2.71 and 3.76 ppm are triplets of triplets; the stronger couplings are to the two protons on position 4 of the 1-pyrroline ring, while the weaker triplet splitting is due to coupling to each other. The resonance at 2.09 ppm is a quintet as the coupling to the two protons on position 3 of the 1-pyrroline ring and the coupling to the two protons on position 5 of the 1-pyrroline ring are approximately equal, so there are four "equivalent" neighbours.

The ^{1}H COSY NMR spectrum (Fig. 7) of **2** has a larger number of signals and a much more complicated spin–spin coupling pattern than the spectrum of **1**. When D_2O was added to a solution of **2** in CD_3OD, the signal at 4.37 ppm began to decrease and the multiplet at 3.6 ppm (corresponding to the signal at 3.3 ppm in dmso-d_6) became a triplet, due to the slow exchange of the amine protons. An hour after the D_2O was added, the quartet at 4.37 ppm was still present; a day later it had completely disappeared. The pattern and intensity of the cross-peaks in the COSY spectrum were used to assign the remaining signals. The signal at 3.3 ppm in dmso-d_6 is obscured by the water peak, but the cross-peaks to the amine protons and the axial and equatorial protons on position 3 of the pyrrolidine rings are observed.

The ^{1}H COSY NMR spectrum of **3** in dmso-d_6 (Fig. S8, Supporting Information †) was used to assign the structure. The 1D ^{1}H NMR spectrum of **3** in CD_3OD was also recorded to determine the structure of the multiplet hidden under the water peak in dmso-d_6. Partial deuterium exchange of the amine protons in CD_3OD solution; and complete exchange in D_2O resulted in a change in the signal due to the protons on position 2 of the pyrrolidine rings from a quartet to a triplet. The rigidity of the molecule results in proton–proton couplings over

Table 6 Nickel(III/II) reduction potentials

Couple	$E_{1/2}$/V (*vs.* NHE)[a]	$E_{1/2}$/V (*vs.* $Fc^{+/0}$)[b]
$\mathbf{1}^{+/0}$	0.950	0.316
$\mathbf{2}^{+/0}$	0.918	
$\mathbf{3}^{+/0}$	0.870	0.033
$\mathbf{4}^{+/0}$		0.220
$\mathbf{5}^{+/0}$		0.311

[a] Solvent: H_2O, supporting electrolyte: $NaClO_4$ (0.1 M) [b] Solvent: *N,N*-dimethylformamide, supporting electrolyte: TBAP (0.1 M)

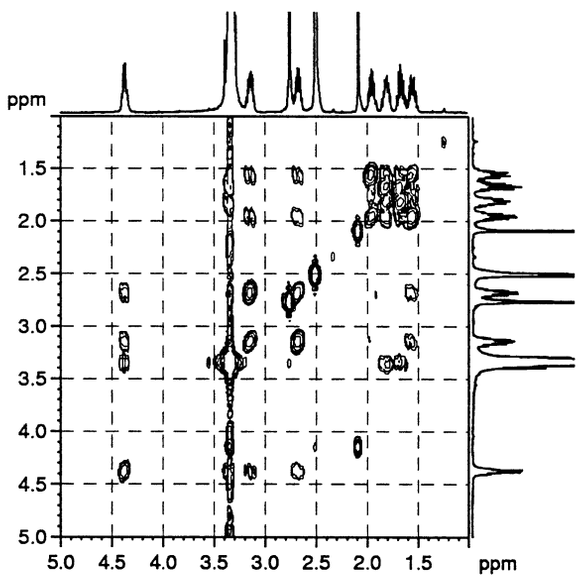

Fig. 7 ^{1}H COSY NMR spectrum of **2** in dmso-d_6. Residual solvent peaks: 2.07 ppm (acetone), 2.48 ppm (dmso-d_5), and 3.32 ppm (water).

quite long paths. There are even weak cross peaks in the COSY ^{1}H NMR spectrum between the resonance due to the protons on positions 1 and 2 of the cyclohexane ring (2.66 ppm), and the resonance due to the protons on position 2 of the pyrrolidine rings (3.38 ppm).

The ^{1}H COSY NMR spectrum of **4** in CD_3OD (Fig. S9, Supporting Information †) did not show exchange of the amine protons with deuterium. When D_2O was added, the quartet due to the amine protons (4.51 ppm) was still visible after 2 d, though it partially overlapped the water peak, which had shifted; therefore, an accurate integration could not be determined. The lack of deuteration of the amines was established by the resonance at 3.72 ppm (protons on position 2 of the pyrrolidine rings), which remained as a quartet. This did not change to a triplet as the equivalent resonances in the spectra of **2** and **3** did on amine deuteration.

There was no evidence of paramagnetic species in the NMR spectra, which showed that the Ni complexes retained their square-planar coordination in solution.

Cyclic voltammetry (CV)

The Ni(III/II) redox couples for **1**–**5** were quasi-reversible at a glassy-carbon working electrode (Table 6); no reversible oxidation was observed for **6**. Not all complexes were soluble in a single solvent, which prevented quantitative comparisons being made amongst the redox properties in the same solvent. At lower scan rates, the Ni(III/II) couple was almost fully reversible, as the scan rate increased quasi-reversible behaviour was apparent as the anodic and cathodic peaks moved farther apart and the relative intensity of the cathodic peak decreased (Fig. S10, Supporting Information †). As the scan rate increased from 10 to 100 mV s^{-1} for **5**, the ratio of the peak currents, i_{pc}/i_{pa}, decreased from 0.91 to 0.46 and the peak-to-peak separation, ΔE_p, increased from 70 to 87 mV. The decrease in the ratio of i_{pc}/i_{pa} is counter-intuitive for a reversible process. However, the Ni(II) complexes are four-coordinate and have a square-planar geometry about the Ni, whereas Ni(III) complexes are usually six-coordinate,[12,64,65] so there is a conformational change when the oxidation state of the nickel changes. At slower scan rates, the scan rate was low compared to the rate of conformational rearrangement, so a single reversible redox couple was observed. As the scan rate increased, the timescale of the experiment became comparable to the rate of conformational rearrangement, *i.e.*, the redox couples for the four-coordinate species and the six-coordinate species started to separate, and the reversibility was lost. Although scan rates of up to 2000 mV s^{-1} were used, distinct redox couples for the four-coordinate and six-coordinate species could not be resolved within the potential window.

The Ni(III/II) reduction potentials determined in this work were similar to those reported for Ni tripeptide complexes in water (0.84–0.96 V *vs.* NHE).[12] With tetrapeptides, peptide amides, and higher order peptides, the values lie in the range 0.79–0.84 V *vs.* NHE.[12] Complexes **1**–**5** had fairly low Ni(III/II) reduction potentials, which indicated that the deprotonated amides were effective at stabilising the Ni(III) oxidation state. The complexes with terminal amine ligands had the lowest Ni(III/II) reduction potentials. The presence of a central benzene bridge made the reduction potential more positive. This was probably due to delocalisation of the negative charge on the deprotonated amide groups into the benzene ring. The most easily oxidised complex was **3**, yet it was complex **2** that underwent oxidative dehydrogenation of the amines during the synthesis. This indicates that factors besides the Ni(II) oxidation potential, such as the strain induced in the ligand upon coordination, influence whether or not the amine groups undergo oxidative dehydrogenation.

Two reversible reductions were observed in the CVs of **5** (Fig. 8(b)) and **6** (Fig. S11(b), Supporting Information †). These

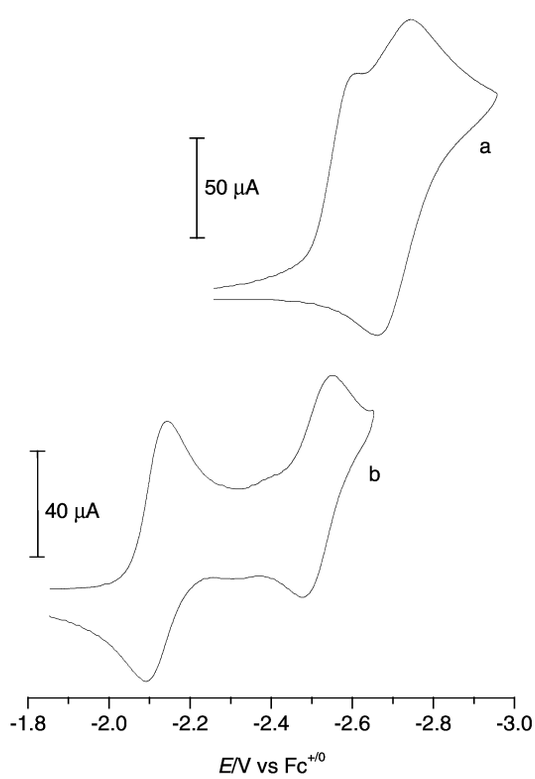

Fig. 8 CV of (a) **I** (3.5 mM) and (b) **5** (5 mM) in DMF, supporting electrolyte: TBAP (0.1 M), glassy-carbon working electrode, at scan rates of (a) 300 mV s^{-1} and (b) 100 mV s^{-1}

reductions were ligand centred; two reductions were also observed in the cyclic voltammograms of the ligands (Fig. 8(a) and Fig. S11(a), Supporting Information), though only the reduction at more negative potential was reversible. The coordination of the ligands to Ni(II) stabilised the reduced forms due to delocalisation of the charge onto the Ni. This stabilisation caused the reduction potentials to shift to more positive values and the first reduction became reversible. These two reductions probably involve the pyridyl rings in the ligand as no reductions, either reversible or irreversible, were observed in the CVs of the pyrrolidine-based ligands **III–V**. A single reversible reduction was observed for **3** and **4** in DMF at −2.808 and −2.680 V *vs.* $Fc^{+/0}$, respectively, and an irreversible reduction of **1** at −2.178 V *vs.* $Fc^{+/0}$. The absence of reductions in the CVs of **IV** and **V** indicates that these reductions are likely to be Ni-based. The CV of **2** was recorded in water (due to its limited solubility in DMF), so it was not possible to examine its redox behaviour with a carbon electrode at the more negative potentials where the other Ni(II) complexes were reduced.

Oxidative dehydrogenation of coordinated amines

The products obtained by the different methods from the reaction of Ni(II) with **III** demonstrated that there were two conditions necessary for oxidative dehydrogenation of the ligand to occur: (i) there must be O_2 present; and (ii) the complex must be dissolved in a basic solution. The syntheses of **2** under Ar were carried out in highly basic solution with OH^- as the base, yet the ^1H NMR spectrum of the product from method 1 did not show evidence of any complexes other than **2**. The success of the synthesis of **1** by method 2 proved that it was not necessary to have a strong base present, since the reaction occurred at pH 10 with the use of the more moderate base, carbonate. It is not possible to say categorically that a high pH value is necessary for the dehydrogenation reaction because the high pH value is necessary to achieve coordination of the deprotonated amide groups to Ni(II). However, the high stability of solutions of **2** in methanol in the presence of O_2 indicates that the base added to deprotonate the amide groups may also be involved in the dehydrogenation.

There are few reports of the oxidative dehydrogenation of amines coordinated to Ni(II). The oxidation of tetrahydrosalen derivatives coordinated to Ni(II) to the dihydrosalen analogues by O_2 has been reported by Böttcher *et. al*.[66] Berkessel, Bats and Schwartz have also reported the oxidative dehydrogenation of a dihydrosalen derivative coordinated to nickel(II) to the salen analogue.[67] Disulfide bond formation, ligand decarboxylation and ligand hydroxylation have been observed in Ni(II)-amide/O_2 systems[9,54,68–71] but this is the first report of amine oxidation in a nickel complex with a mixed amine–amide ligand.

In the oxidative dehydrogenation of the tetrahydrosalen, there was evidence that the mechanism involved O_2 binding to the Ni(II).[66] Higher oxidation states of nickel have also been implicated as intermediates in ligand oxidation in some Ni(II)–amide/O_2 systems.[9,69,70] The oxidative dehydrogenation of **III** is postulated to occur by a mechanism involving O_2 binding to the Ni(II), leading to the formation of a higher-oxidation-state Ni species followed by an intramolecular oxidative dehydrogenation of an amine group with concomitant reduction back to Ni(II). The oxidation of the two amine groups to imines observed would mean that this happens twice for each molecule. This is unlike the oxidative dehydrogenation of the tetrahydrosalen and dihydrosalen ligands[66,67] where only a single amine group was oxidised.

The mechanism of DNA damage by Ni(II)–peptide complexes is postulated to involve their oxidation to complexes in higher oxidation states.[1,2,6,10] The relatively low Ni(III/II) reduction potentials showed that deprotonated amide donor groups were effective at stabilising Ni(III). The O_2 oxidation of the Ni complex of **III** indicates that with deprotonated amide nitrogen coordination, the higher oxidation states of Ni are accessible using relatively mild oxidants. This may have relevance as a biomimetic reaction leading to the biological oxidation of DNA species.

Acknowledgements

Our thanks to Dr Ming Xie and Dr Ian Luck from the NMR facility in the School of Chemistry, University of Sydney for recording the 400 MHz NMR spectra. This work has been supported by funding from Australian Research Council (ARC) grants, an ARC RIEFP grant for an X–ray diffractometer, and an APA scholarship to C. L. W.

References

1 Q. Liang, D. C. Ananias and E. C. Long, *J. Am. Chem. Soc.*, 1998, **120**, 248.
2 D. P. Mack and P. B. Dervan, *J. Am. Chem. Soc.*, 1990, **112**, 4604.
3 Q. Liang, P. D. Eason and E. C. Long, *J. Am. Chem. Soc.*, 1995, **117**, 9625.
4 D. F. Shullenberger, P. D. Eason and E. C. Long, *J. Am. Chem. Soc.*, 1993, **115**, 11038.
5 M. Footer, M. Egholm, S. Kron, J. M. Coull and P. Matsudaira, *Biochemistry*, 1996, **35**, 10673.
6 C. Harford, S. Narindrasorasak and B. Sarkar, *Biochemistry*, 1996, **35**, 4271.
7 D. P. Mack and P. B. Dervan, *Biochemistry*, 1992, **31**, 9399.
8 M. Nagaoka, M. Hagihara, J. Kuwahara and Y. Sugiura, *J. Am. Chem. Soc.*, 1994, **116**, 4085.
9 C. J. Burrows, R. J. Perez, J. G. Muller and S. E. Rokita, *Pure Appl. Chem.*, 1998, **70**, 275.
10 E. C. Long, *Acc. Chem. Res.*, 1999, **32**, 827.
11 F. P. Bossu and D. W. Margerum, *J. Am. Chem. Soc.*, 1976, **98**, 4003.
12 F. P. Bossu and D. W. Margerum, *Inorg. Chem.*, 1977, **16**, 1210.
13 D. J. Barnes, R. L. Chapman, R. S. Vagg and E. C. Watton, *J. Chem. Eng. Data*, 1978, **23**, 349.
14 R. R. Fenton, F. S. Stephens and R. S. Vagg, *J. Coord. Chem.*, 1991, **23**, 291.
15 R. L. Chapman and R. S. Vagg, *Inorg. Chim. Acta*, 1979, **33**, 227.
16 M. Mulqi, F. S. Stephens and R. S. Vagg, *Inorg. Chim. Acta*, 1981, **53**, L91.
17 D. J. Barnes, R. L. Chapman, F. S. Stephens and R. S. Vagg, *Inorg. Chim. Acta*, 1981, **51**, 155.
18 M. Mulqi, F. S. Stephens and R. S. Vagg, *Inorg. Chim. Acta*, 1981, **52**, 73.
19 R. L. Chapman, F. S. Stephens and R. S. Vagg, *Inorg. Chim. Acta*, 1981, **52**, 161.
20 F. S. Stephens and R. S. Vagg, *Inorg. Chim. Acta*, 1982, **57**, 9.
21 M. Mulqi, F. S. Stephens and R. S. Vagg, *Inorg. Chim. Acta*, 1982, **62**, 215.
22 M. Mulqi, F. S. Stephens and R. S. Vagg, *Inorg. Chim. Acta*, 1982, **63**, 197.
23 F. S. Stephens and R. S. Vagg, *Inorg. Chim. Acta*, 1984, **90**, 17.
24 F. S. Stephens and R. S. Vagg, *Inorg. Chim. Acta*, 1986, **120**, 165.
25 M.-J. Jun and C. F. Liu, *Inorg. Chem.*, 1975, **14**, 2310.
26 M.-J. Jun and C. F. Liu, *Inorg. Chim. Acta*, 1975, **15**, 111.
27 B.-W. Lee, J.-H. Park, D.-K. Son, B.-G. Kim, C.-E. Oh and M.-K. Doh, *Bull. Korean Chem. Soc.*, 1999, **20**, 749.
28 M. J. Alcon, E. Gutierrez-Puebla, M. Iglesias, M. A. Monge and F. Sanchez, *Inorg. Chim. Acta*, 2000, **306**, 117.
29 M. J. Alcon, M. Iglesias, F. Sanchez and I. Viani, *J. Organomet. Chem.*, 2000, **601**, 284.
30 A. Berger, J. Kurtz and E. Katchalski, *J. Am. Chem. Soc.*, 1954, **76**, 5552.
31 R. R. Fenton, unpublished work, 1990.
32 Molecular Structure Corporation teXsan: crystal structure analysis package, Molecular Structure Corporation, 3200 Research Forest Drive, The Woodlands, TX, USA, 1997–1998, 1985 & 1992.
33 D. T. Cromer and J. T. Waber, *International Tables for X-ray Crystallography*, The Kynoch Press, Birmingham, 1974.
34 J. A. Ibers and W. C. Hamilton, *Acta Crystallogr.*, 1964, **17**, 781.
35 D. C. Creagh and W. J. McAuley, *International Tables for Crystallography*, ed. A. J. C. Wilson, Kluwer Academic Publishers, Dordrecht, 1992.
36 D. C. Creagh and J. H. Hubbell, *International Tables for Crystallography*, ed. A. J. C. Wilson, Kluwer Academic Publishers, Dordrecht, 1992.

37 Molecular Structure Corporation teXsan for Windows: Single Crystal Structure Analysis Software, Molecular Structure Corporation, 3200 Research Forest Drive, The Woodlands, TX, USA, 1997–1998.
38 Bruker SMART, SAINT and XPREP. Area detector control and data integration and reduction software, Bruker Analytical X-ray Instruments Inc., Madison, WI, USA, 1995.
39 G. M. Sheldrick, SADABS. Empirical absorption correction program for area detector data, University of Göttingen, Germany, 1996.
40 P. T. Beurskens, G. Admiraal, G. Buerskens, W. P. Bosman, S. Garcia-Granda, R. O. Gould, J. M. M. Smits, and C. Smykalla, PATTY. The DIRDIF program system, Technical Report of the Crystallography Laboratory, University of Nijmegen, The Netherlands, 1992.
41 P. T. Beurskens, G. Admiraal, G. Beurskens, W. P. Bosman, R. de Gelder, R. Israel, and J. M. M. Smits, DIRDIF94. The DIRDIF-94 program system, Technical Report of the Crystallography Laboratory, University of Nijmegen, The Netherlands, 1994.
42 G. M. Sheldrick, SHELXS97. Program for crystal structure solution, University of Göttingen, Germany, 1997.
43 G. M. Sheldrick, SHELXL97. Program for crystal structure refinement, University of Göttingen, Germany, 1997.
44 H. D. Flack, *Acta Crystallogr., Sect. A*, 1983, **39**, 876.
45 G. Bernadelli and H. D. Flack, *Acta Crystallogr., Sect. A*, 1985, **41**, 500.
46 G. Davenport and H. Flack, in LSQPL Xtal3.6 System, ed. S. R. Hall, D. J. du Boulay and R. Olthof-Hazekamp, University of Western Australia, Perth, 1999.
47 A. Altomare, M. Cascarano, C. Giacovazzo and A. Guagliardi, *J. Appl. Crystallogr.*, 1993, **26**, 343.
48 Bruker XSHELL. Graphical interface for crystal structure refinement, Bruker Analytical X-ray Intruments Inc., Madison, WI, USA, 1995.
49 L. J. Bellamy, *The Infra-red Spectra of Complex Molecules*, Methuen and Co. Ltd., London, 1959.
50 G. Galaverna, R. Corradini, A. Dossena, R. Marchelli and F. Dallavalle, *Chirality*, 1996, **8**, 189.
51 W.-H. Leung, J.-X. Ma, V. W.-W. Yam, C.-M. Che and C.-K. Poon, *J. Chem. Soc., Dalton Trans.*, 1991, 1071.
52 C. K. Johnson, ORTEP: ORTEPII Report ORNL-5138, Oak Ridge National Laboratory, Oak Ridge, TN, 1976.
53 T. J. Collins, T. R. Nichols and E. S. Uffelman, *J. Am. Chem. Soc.*, 1991, **113**, 4708.
54 W. Bal, M. I. Djuran, D. W. Margerum, E. T. Gray Jr., M. A. Mazid, R. T. Tom, E. Nieboer and P. J. Sadler, *J. Chem. Soc., Chem. Commun.*, 1994, 1889.
55 H. C. Freeman, J. M. Guss and R. L. Sinclair, *Acta Crystallogr., Sect. B*, 1978, **34**, 2459.
56 H. C. Freeman, J. M. Guss and R. L. Sinclair, *Chem. Commun.*, 1968, 485.
57 T. Kawamoto, H. Kuma and Y. Kushi, *Bull. Chem. Soc. Jpn.*, 1997, **70**, 1599.
58 G. Brewer, P. Kamaras, L. May, S. Prytkhov and M. Rapta, *Inorg. Chim. Acta*, 1998, **279**, 111.
59 H. Keypour, S. Salehzadeh, R. G. Pritchard and R. V. Parish, *Trans. Met. Chem.*, 1998, **23**, 605.
60 A. Garoufis, S. Kasselouri, C.-A. Mitsopoulou, J. Sletten, C. Papadimitriou and N. Hadjiliadis, *Polyhedron*, 1998, **18**, 39.
61 A. Garoufis, S. Kasselouri, C. P. Raptopoulou and A. Terzis, *Polyhedron*, 1998, **18**, 585.
62 E. Kwiatkowski, M. Klein and G. Romanowski, *Inorg. Chim. Acta*, 1999, **293**, 115.
63 E. Szlyk, A. Wojtczak, E. Larsen, A. Surdykowski and J. Neumann, *Inorg. Chim. Acta*, 1999, **293**, 239.
64 C. K. Murray and D. W. Margerum, *Inorg. Chem.*, 1982, **21**, 3501.
65 R. Machida, E. Kimura and Y. Kushi, *Inorg. Chem.*, 1986, **25**, 3461.
66 A. Böttcher, H. Elias, L. Mueller and H. Paulus, *Angew. Chem., Int. Ed. Engl.*, 1992, **31**, 623.
67 A. Berkessel, J. W. Bats and C. Schwarz, *Angew. Chem., Int. Ed. Engl.*, 1990, **29**, 106.
68 E. B. Paniago, D. C. Weatherburn and D. W. Margerum, *Chem. Commun.*, 1971, 1427.
69 F. P. Bossu, E. B. Paniago, D. W. Margerum, S. T. Kirksey Jr. and J. L. Kurtz, *Inorg. Chem.*, 1978, **17**, 1034.
70 S. A. Ross and C. J. Burrows, *Inorg. Chem.*, 1998, **37**, 5358.
71 D. Chen, R. J. Motekaitis and A. E. Martell, *Inorg. Chem.*, 1991, **30**, 1396.